

# On the relic abundance of light photinos

Daniel J. H. Chung\*

*Department of Physics and Enrico Fermi Institute  
The University of Chicago, Chicago, Illinois 60637, and  
NASA/Fermilab Astrophysics Center  
Fermi National Accelerator Laboratory, Batavia, Illinois 60510*

Glennys R. Farrar†

*Department of Physics and Astronomy  
Rutgers University, Piscataway, New Jersey 08855*

Edward W. Kolb‡

*NASA/Fermilab Astrophysics Center  
Fermi National Accelerator Laboratory, Batavia, Illinois 60510, and  
Department of Astronomy and Astrophysics and Enrico Fermi Institute  
The University of Chicago, Chicago, Illinois 60637*

We solve the coupled Boltzmann equation for the system of light photinos interacting with pions and  $R^0$ 's (the gluon-gluino bound state) to determine the relic abundance of light photinos in the light gaugino scenario. Cosmology bounds the ratio  $r$  of the  $R^0$  mass to the  $\tilde{\gamma}$  mass to be less than about 1.8. We also use a model Lagrangian embodying crossing symmetry between the  $R^0 \leftrightarrow \tilde{\gamma}\pi\pi$  and  $R^0\pi \leftrightarrow \tilde{\gamma}\pi$  reactions to identify cosmologically favored regions of  $R^0$  lifetime as a function of  $R^0$  and  $\tilde{\gamma}$  masses.

PACS number(s): 95.35.+d, 14.80.Ly, 98.80.Cq

---

\*Electronic mail: djchung@yukawa.uchicago.edu

†Electronic mail: farrar@physics.rutgers.edu

‡Electronic mail: rocky@rigoletto.fnal.gov

## I. INTRODUCTION

In supersymmetric (SUSY) models without dimension-3 supersymmetry-breaking operators, gauginos are massless at the tree level and obtain non-zero masses solely from radiative corrections [1,2,3]. This means that the gluino is light and the lightest neutralino is nearly a pure photino. Farrar [4,5,6] found that the light gluinos and photinos arising from this scenario are consistent with the present experimental constraints.<sup>2</sup> Although it was once generally believed that the light gaugino scenario conflicted with the cosmological relic abundance constraints, Farrar and Kolb [9] showed that the previous constraint calculations neglected the reaction channels which really control the relic abundance. Indeed, based on some simple estimates, they concluded that a light photino (the relic stable particle in the present SUSY scenario) might be a significant dark matter candidate. However, their estimates were based on the approximation that only a single reaction dominates the relic abundance evolution and that the abundance evolution stops exactly when the dominant reaction rate becomes less than the Hubble expansion rate (the “sudden” approximation).

In the present paper, we calculate the cosmological constraints for this scenario of light gluinos and photinos more carefully by integrating the Boltzmann equations for the relic abundance. The three most important reactions determining the photino abundance are  $R^0\pi^\pm \leftrightarrow \pi^\pm\tilde{\gamma}$ ,  $R^0 \rightarrow \pi^+\pi^-\tilde{\gamma}$ , and  $R^0R^0 \rightarrow X$ . The first two are related by crossing symmetry. In the limit that left and right handed squark masses are equal, such that charge conjugation is a good symmetry of the theory, and ignoring the momentum

---

<sup>2</sup>The recent ALPEH claim to exclude light gluinos [7] assigns a  $1\sigma$  theoretical systematic error based on varying the renormalization scale over a small range. Taking a more generally accepted range of scale variation and accounting for the large sensitivity to hadronization model, the ALEPH systematic uncertainty is comparable to that of other experiments and does not exclude light gluinos [8].

dependence of the matrix elements, this crossing relation indicates that both reactions may play an important role instead of one reaction dominating over the other. We use the results of our model calculations to help identify the cosmologically most promising values for phenomenologically important parameters such as the  $R^0$  lifetime, which can help in laboratory searches.

Let us now briefly introduce the relevant features of our SUSY scenario. Supersymmetric models with acceptable SUSY breaking phenomenology are generically invariant under a global chiral symmetry called  $R$ -invariance.  $R$ -invariance is broken spontaneously by the vacuum expectation values of the Higgs fields associated with electroweak symmetry breaking, and by tree-level gaugino masses if they are present.  $R$ -parity is the possible discrete remnant of this broken continuous symmetry. Under  $R$ -parity, the gluino, photino, and squarks are odd, while ordinary particles (e.g., gauge and Higgs bosons and quarks) are even.  $R$ -parity, which we shall assume is an unbroken symmetry, ensures that the lightest  $R$ -odd particle is stable and prevents unacceptably rapid proton decay. Thus, in calculating the relic density in SUSY, one first identifies the lightest  $R$ -odd particle which usually is the lightest supersymmetric particle (LSP). Although the gluino may be the lightest particle in our scenario, it cannot exist in isolation today because it is not a color singlet. Bound to a gluon or a color-octet system of quarks and/or anti-quarks, it forms a color singlet hadron. The lightest of these is expected to be a gluon-gluino bound state called  $R^0$ , whose mass should be comparable to that of the lightest glueball [4, 5]. Because this is most likely heavier than the photino, it is the photino which acquires the role usually taken on by the LSP even though it may be heavier than the gluino.<sup>3</sup>

---

<sup>3</sup> In some SUSY-breaking models only the gluino is massless at tree level, while other gauginos have large masses. In this case the  $R^0$  could be the LSP and relic  $R^0$ 's would be the SUSY dark matter candidate. The dark matter density can be approximated as in [12], accounting for only the  $R^0 R^0$  self-

Table I: A list of SUSY mass parameters and ranges used in the analysis.

Particle	Mass Notation	Min.(GeV)	Max.(GeV)
photino( $\tilde{\gamma}$ )	$m$	0.2	1.4
$R^0(\tilde{g})$	$M$	1	2
squark	$M_S$	50	300

Since freeze out occurs after the color confinement phase transition, only gluinos bound in color singlet states are relevant to our calculation. Among the bound states containing a gluino ( $R$ -hadrons), the  $R^0$  is expected to react most prominently with the photino because other  $R$ -hadrons are significantly heavier and thus Boltzmann suppressed at the relevant temperatures. Furthermore, most of the other  $R$ -odd states will contribute to the photino abundance only after having decayed to an  $R^0$  channel. Thus, the photino relic abundance will be determined primarily by the reactions involving an  $R^0$ , a  $\tilde{\gamma}$ , and non-SUSY particles.

In our scenario, the photino abundance depends crucially on interactions of hadrons after the confinement phase transition, causing complications distinct from conventional scenarios where the freeze out occurs above the confinement transition temperature. In particular, we are only able to make reasonable guesses for the relevant reaction rates because of incalculable long-distance QCD effects and our lack of direct experimental data for the reaction rates of interest. Fortunately, we are still able to make useful predictions regarding the  $R^0$  and  $\tilde{\gamma}$  masses and  $R^0$  lifetime.

The relic abundance of photinos depends mainly upon the masses of  $\tilde{\gamma}$  and  $R^0$ , the cross sections for  $R^0\pi \rightarrow \pi\tilde{\gamma}$  and  $R^0R^0 \rightarrow X$  (where  $X$  denote any strongly interacting annihilation. This gives  $\Omega_{R^0}h^2 \lesssim 10^{-7}$ . That is, due to their strong interactions,  $R^0$ 's stay in thermal equilibrium too long for their abundance to freeze out at a non-negligible value. Thus such SUSY-breaking scenarios do not provide a natural visible sector dark matter candidate unless the gravitino has acceptable properties.

light species of particles such as the pions), and the decay rates for  $R^0 \rightarrow \tilde{\gamma}\pi\pi$  and  $R^0 \rightarrow \tilde{\gamma}\pi$ . The mass parameter space that will be explored in this calculation is justified in Refs. [2] and [5] and is similar to that discussed in Ref. [9]. The relevant mass parameters and their plausible ranges are shown in Table I. The gluino mass itself is unimportant, except insofar as it influences the  $R^0$  mass,  $M$ . The relevant squark mass denoted  $M_S$  is a charge-weighted average of up- and down-squark masses. See Ref. [10] for squark mass limits in the light gluino scenario.

In order to express some of the formulae showing numerical estimates concisely, we also define the following dimensionless ratios:

$$\mu_8 \equiv \frac{m}{0.8 \text{ GeV}}; \quad \mu_S \equiv \frac{M_S}{100 \text{ GeV}}; \quad r \equiv \frac{M}{m}. \quad (1)$$

As pointed out in Ref. [9], the relic abundance is particularly sensitive to the parameter  $r$ . Note that because of the ranges we adopt, given in Table I, the range of  $r$  we explore is constrained for a fixed value of  $m$ .

In the next section, we discuss the Boltzmann equation and some simplifying assumptions used to calculate the present photino abundance (density). In Section III, we briefly describe the reactions that are included in the simplified Boltzmann equations. The results of the integration are presented and analyzed in Section IV. In Section V we develop an effective Lagrangian description of the interaction between  $R^0$ ,  $\tilde{\gamma}$  and pions which embodies the symmetries of the underlying theory as well as the crossing and chiral-perturbation theory constraints. Ignoring the possibility that a nearby  $R_\pi$  resonance produces a strong momentum dependence, the two dominant reactions controlling the  $\tilde{\gamma}$  abundance are determined by a single parameter. Using this approximation, we obtain an estimate of the cosmologically favored lifetime range of the  $R^0$  as a function of its mass. We summarize our results in Section VI. In an appendix, we analyze the possible resonance enhancement of the  $R^0\pi \rightarrow \tilde{\gamma}\pi$  cross section using a Breit-Wigner

model.

## II. THE BOLTZMANN EQUATIONS

The standard method of calculating the relic abundance is to integrate a simplified form of the Boltzmann equations [11,12]. We now briefly remind the reader of the general formulation. One can write the Boltzmann equations<sup>4</sup> for the evolution of the particle density  $n_j$  as

$$\frac{dn_j}{dt} + 3Hn_j = - \sum_i \frac{\langle W_{jA_{ji} \rightarrow B_{ji}} V^{n(A_{ji})} \rangle}{\prod_{\lambda \in B_{ji}} n_\lambda^{eq}} \times \left( n_j \prod_{k \in A_{ji}} n_k \prod_{\lambda \in B_{ji}} n_\lambda^{eq} - n_j^{eq} \prod_{k \in A_{ji}} n_k^{eq} \prod_{\lambda \in B_{ji}} n_\lambda \right) \quad (2)$$

where  $H$  is the usual Hubble expansion rate,  $A_{ji}$  and  $B_{ji}$  are sets of particle species relevant to the evolution of species  $j$ , and the summation is over all the reactions of the form  $jA_{ji} \rightarrow B_{ji}$ . We have defined the thermal averaged transition rate as

$$\langle W_{jA_{ji} \rightarrow B_{ji}} V^{n(A_{ji})} \rangle \equiv \frac{\int [dp] (2\pi)^4 \delta^{(4)} \left( \sum_k p_k \right) |T_{jA_{ji} \rightarrow B_{ji}}|^2 \exp\left(- \sum_{\lambda \in j, A_{ji}} E_\lambda / T\right)}{\prod_{p \in j, A_{ji}} (n_p^{eq} / g_p)} \quad (3)$$

$$[dp] \equiv \prod_{k \in j, A_{ji}, B_{ji}} \frac{d^3 p_k}{(2\pi)^3 2E_k} \quad (4)$$

$$n_x^{eq} \equiv g_x \int \frac{d^3 p_x}{(2\pi)^3} \exp(-E_x / T) \quad (5)$$

where  $n_x^{eq}$  is the equilibrium density,<sup>5</sup>  $g_x$  counts the spin multiplicity, and  $|T_{jA_{ji} \rightarrow B_{ji}}|^2$  represents the spin averaged transition amplitude squared.<sup>6</sup> In the case of one initial

<sup>4</sup>As usual, we have used the assumption of molecular chaos to obtain a closed set of equations.

<sup>5</sup>As usual, the particle described by this equilibrium density is assumed to have mass much greater than the temperature.

<sup>6</sup>The  $W$  symbol actually represents the number of transitions per unit time when all the initial state

state particle,  $\langle W_{jA_{ji} \rightarrow B_{ji}} V^{n(A_{ji})} \rangle$  evaluates to a decay rate, whereas in the case when there are two initial state particles,  $\langle W_{jA_{ji} \rightarrow B_{ji}} V^{n(A_{ji})} \rangle$  evaluates to the familiar  $\langle \sigma v \rangle$  of a scattering reaction. For example, in the case of a photino density evolution determined only by the reaction  $\tilde{\gamma}\tilde{\gamma} \leftrightarrow X$ , the density labels become  $j = \tilde{\gamma}$ ,  $A_{ji} = A_{\tilde{\gamma}\tilde{\gamma}} = \{\tilde{\gamma}\}$ , and  $B_{ji} = B_{\tilde{\gamma}\tilde{\gamma}} = \{X\}$ ; the summation in  $i$  reduces to a sum over one element (the annihilation channel); and the transition rate per unit fluxes becomes  $\langle W_{\tilde{\gamma}\tilde{\gamma} \rightarrow X} V \rangle = \langle v\sigma(\tilde{\gamma}\tilde{\gamma} \rightarrow X) \rangle$ . With the usual assumption that the final products  $X$  are in equilibrium, Eq. (5) reduces to the familiar equation (see, for example, pg. 120 of Ref. [12])

$$\frac{dn_{\tilde{\gamma}}}{dt} + 3Hn_{\tilde{\gamma}} = -\langle v\sigma(\tilde{\gamma}\tilde{\gamma} \rightarrow X) \rangle (n_{\tilde{\gamma}}^2 - n_{\tilde{\gamma}}^{eq2}). \quad (6)$$

Note that Eq. (2) assumes that the fluid is rare enough to disregard degenerate pressure effects and assumes that time reversal is a good symmetry. More specifically, time reversal symmetry is encoded in the following identity used in obtaining Eq. (2):

$$\langle W_{jA_{ji} \rightarrow B_{ji}} V^{n(A_{ji})} \rangle = \langle W_{B_{ji} \rightarrow jA_{ji}} V^{n(B_{ji})-1} \rangle \frac{\prod_{\lambda \in B_{ji}} n_{\lambda}^{eq}}{n_j^{eq} \prod_{\lambda \in A_{ji}} n_{\lambda}^{eq}} \quad (7)$$

Before we can utilize Eq. (2) to determine the relic abundance of the photinos, we need to specify our model of  $H$  and the reactions that are involved. Because the universe is radiation dominated for the temperatures of interest, the equation of state is taken to be  $3 \times (\text{pressure}) = (\text{energy density})$  and any possible spatial curvature is neglected. We also use equilibrium statistics with the number of relativistic degrees of freedom set to  $g_* = 10.75$ . The resulting equation for the Hubble expansion rate as a function of temperature is  $H = \sqrt{8\pi^3 g_*/90} (T^2/m_{pl})$ , where  $m_{pl}$  is the Planck mass. The reactions that can enter the Boltzmann equations include  $\tilde{\gamma}R^0 \leftrightarrow X$ ,  $\tilde{\gamma}\tilde{\gamma} \leftrightarrow X$ ,  $R^0R^0 \leftrightarrow X$ ,  $\tilde{\gamma}\pi \leftrightarrow R^0$ ,  $\tilde{\gamma}\pi\pi \leftrightarrow R^0$ , and  $\tilde{\gamma}\pi \leftrightarrow R^0\pi$  ( $X$ 's denote any allowed light products that interact strongly or electromagnetically).

reactants have equal unit flux. The  $V$  symbol represents the characteristic spatial volume of interaction and the power  $n$  is the number of initial state particles minus one.

In general, Eq. (2) generates a set of coupled nonlinear differential equations which can be solved numerically. However, instead of considering all the particle densities as unknowns, we can simplify the situation with the good approximation that the particle densities whose equilibrating chemical reaction rate is large compared to the Hubble expansion rate follow equilibrium densities of the form Eq. (5). This, in fact, is the justification for our Boltzmann evolution's initial condition which is to start all species at equilibrium densities given by Eq. (5). With this expectation, we replace the  $X$  and the  $\pi$  densities in the Boltzmann equation with the equilibrium densities. We are then left to consider only the  $R^0$  and the  $\tilde{\gamma}$  densities as functions that require solutions.

To understand which reactions will be most important in our system, we first recast Eq. (2) into the dimensionless form

$$\frac{x}{Y_j} \frac{d}{dx} Y_j = - \sum_i \frac{\langle W_{jA_{ji} \rightarrow B_{ji}} V^{n(A_{ji})} \rangle \prod_{\lambda \in A_{ji}} n_\lambda^{eq}}{H(x)} \left( \frac{\prod_{\lambda \in A_{ji}} Y_\lambda}{\prod_{\lambda \in A_{ji}} Y_\lambda^{eq}} - \frac{Y_j^{eq} \prod_{k \in B_{ji}} Y_k}{Y_j \prod_{k \in B_{ji}} Y_k^{eq}} \right) \quad (8)$$

where  $Y_r = n_r/s$ ,  $s$  is the entropy per comoving volume given by  $s \approx (2\pi^2/45)g_* m^3/x^3$  (entropy conservation is assumed), and  $x = m/T$ . Note that we can interpret the numerator above  $H(x)$  to be the reaction rate per unit density of  $j$ 's. For the purpose of illustration, suppose two reactions named  $a$  and  $b$  are governing the evolution of  $j$  particles and the reaction rates corresponding to them are labeled  $R_a$  and  $R_b$ . The evolution equation in the form of Eq. (8) then becomes

$$\frac{x}{Y_j} \frac{dY_j}{dx} = - \frac{R_a(x)}{H(x)} (\text{ratios a}) - \frac{R_b(x)}{H(x)} (\text{ratios b}) \quad (9)$$

where the ‘‘ratios’’ refer to the terms consisting of density ratios. Suppose further that we are at a time when  $R_a(x)/H(x) \ll 1$  while  $R_b(x)/H(x) \gg 1$ . Then as long as the ‘‘ratios a’’ and ‘‘ratios b’’ are comparable in value, reaction  $a$  can be neglected during this period of evolution. Furthermore, if the final products of reaction  $b$  are in equilibrium, the  $j$  particle density will follow the equilibrium density as long as reaction  $b$  dominates. With



such reasoning, Ref. [9] argues that  $\tilde{\gamma}R^0 \leftrightarrow X$  and  $\tilde{\gamma}\tilde{\gamma} \leftrightarrow X$  reactions play a negligible role compared to  $R^0R^0 \leftrightarrow X$ ,  $\tilde{\gamma}\pi \leftrightarrow R^0\pi$ , and  $\tilde{\gamma}\pi \leftrightarrow R^0$  in keeping the  $R^0$  and the  $\tilde{\gamma}$  densities in equilibrium near the time of  $\tilde{\gamma}$  freeze out. In our present work, we shall neglect only the weakest of the relevant reactions,  $\tilde{\gamma}R^0 \leftrightarrow X$ .<sup>7</sup>

The Boltzmann equations relevant to calculating the  $\tilde{\gamma}$  abundance thus reduce to a pair of coupled differential equations containing terms corresponding to the set of reactions  $\tilde{\gamma}\pi\pi \leftrightarrow R^0$ ,  $\tilde{\gamma}\pi \leftrightarrow R^0$ ,  $\tilde{\gamma}\pi \leftrightarrow R^0\pi$ ,  $R^0R^0 \leftrightarrow X$ ,  $\tilde{\gamma}\tilde{\gamma} \leftrightarrow X$ :

$$\frac{x}{Y_{\tilde{\gamma}}} \frac{dY_{\tilde{\gamma}}}{dx} = -\frac{R_{tot}}{H} \left( 1 - \frac{Y_{\tilde{\gamma}}^{eq} Y_{R^0}}{Y_{\tilde{\gamma}} Y_{R^0}^{eq}} \right) - \frac{2\langle W_{\tilde{\gamma}\tilde{\gamma} \rightarrow X} V \rangle n_{\tilde{\gamma}}^{eq}}{H} \left( \frac{Y_{\tilde{\gamma}}^{eq}}{Y_{\tilde{\gamma}}} \right) \left( \frac{Y_{\tilde{\gamma}}^2}{Y_{\tilde{\gamma}}^{eq2}} - 1 \right) \quad (10)$$

$$\begin{aligned} \frac{x}{Y_{R^0}} \frac{dY_{R^0}}{dx} = & -\frac{R_{tot}}{H} \left( \frac{Y_{\tilde{\gamma}}^{eq}}{Y_{R^0}^{eq}} \right) \left( 1 - \frac{Y_{\tilde{\gamma}} Y_{R^0}^{eq}}{Y_{\tilde{\gamma}}^{eq} Y_{R^0}} \right) \\ & - \frac{2\langle W_{R^0R^0 \rightarrow X} V \rangle n_{R^0}^{eq}}{H(x)} \left( \frac{Y_{R^0}^{eq}}{Y_{R^0}} \right) \left( \frac{Y_{R^0}^2}{Y_{R^0}^{eq2}} - 1 \right) \end{aligned} \quad (11)$$

$$R_{tot} \equiv (\langle W_{\tilde{\gamma}\pi \rightarrow R^0} V \rangle n_{\pi}^{eq} + \langle W_{\tilde{\gamma}\pi\pi \rightarrow R^0} V^2 \rangle n_{\pi}^{eq} n_{\pi}^{eq} + N \langle W_{\tilde{\gamma}\pi \rightarrow \pi R^0} V \rangle n_{\pi}^{eq}). \quad (12)$$

The factor of  $N$  comes from summing over the isospins of  $\pi$ . In the next section, we argue that only  $\pi^{\pm}$  should be included in  $\tilde{\gamma}\pi \rightarrow \pi R^0$ , resulting in  $N = 2$ .<sup>8</sup>

Before we move on to discuss the transition rates, let us clarify the term “freeze out time” used in this paper, particularly in Section IV. In agreement with what will be revealed in the next section, suppose that the self-annihilation term in Eq. (10) can be neglected compared to the term associated with  $R_{tot}$ . When  $R_{tot}/H$  becomes much less than unity and continues decreasing sufficiently fast to keep the right hand side of Eq. (10) much less than unity despite the increases in the magnitude of the term multiplying  $R_{tot}/H$ , the fractional change in  $Y_{\tilde{\gamma}}$  becomes negligible. This is then a sufficient condition for the number of  $\tilde{\gamma}$ 's becoming approximately constant (freezing out). We shall use the

<sup>7</sup>We have checked numerically that this reaction plays a negligible role.

<sup>8</sup>The choice  $N = 3$  was implicit in the treatment in Ref. [9].

term freeze out time to refer to the approximate time at which  $R_{tot}/H$  becomes much less than unity.

### III. THE TRANSITION RATES

Transition amplitudes for  $R^0$ ,  $\tilde{\gamma}$ , and pions depend on hadronic matrix elements of four-fermion effective operators of the form  $\tilde{g}\tilde{\gamma}\bar{q}q$ , obtained by integrating out the squark degree of freedom. Since only a small number of fundamental short-distance operators underly all the transition amplitudes of interest, crossing symmetry can be used to relate transition amplitudes for some of the reactions. Due to the possibly strong momentum dependence of the amplitudes, however, this proves to be of limited utility. This is discussed in Section V.

The particles  $R^0$  and  $\tilde{\gamma}$  are charge conjugation even and odd, respectively [6]. Thus, if charge conjugation were a good symmetry of the interaction, pions coupling an  $R^0$  to a  $\tilde{\gamma}$  would have to be in a C-odd state. However, C invariance is violated by the mass-splitting between  $L$  and  $R$ -chiral squarks (superpartners of the left and right chiral quarks). This mass splitting is a model dependent aspect of SUSY breaking. Fortunately, as we will see, our analysis is quite insensitive to the extent of C violation.

We now present expressions for the transition rates to be used in Eq. (10):  $\langle W_{\tilde{\gamma}\pi\rightarrow R^0} V \rangle n_{\pi}^{eq}$ ,  $\langle W_{\tilde{\gamma}\pi\rightarrow\pi R^0} V \rangle n_{\pi}^{eq}$ ,  $\langle W_{\tilde{\gamma}\pi\pi\rightarrow R^0} V^2 \rangle n_{\pi}^{eq} n_{\pi}^{eq}$ ,  $\langle W_{R^0 R^0\rightarrow X} V \rangle n_{R^0}^{eq}$ , and  $\langle W_{\tilde{\gamma}\tilde{\gamma}\rightarrow X} V \rangle n_{\tilde{\gamma}}^{eq}$ . We shall see that the resulting expressions do not differ significantly from those of Ref. [9] even though the issue of charge conjugation symmetry is ignored in that reference.

#### A. The $\tilde{\gamma} - R^0$ conversion reaction $\tilde{\gamma}\pi \rightarrow \pi R^0$

If charge conjugation invariance were exact, the neutral pion channel would be ab-

sent as it necessarily violates C. However, even if C is maximally violated, the condition  $\sigma(\tilde{\gamma}\pi^0 \rightarrow \pi^0 R^0) \ll \sigma(\tilde{\gamma}\pi^\pm \rightarrow \pi^\pm R^0)$  still applies because the  $\tilde{\gamma}R^0 q\bar{q}$  coupling is proportional to the quark charge, causing a first order cancelation to occur in the case of a neutral  $\pi^0$ . Thus we can ignore the neutral channel without serious impact on the quantitative results. In order to avoid any thermal averaging complications that may arise from threshold effects, we estimate the cross section for  $R^0\pi^\pm \rightarrow \pi^\pm\tilde{\gamma}$  instead of the cross section for the inverse reaction. The cross section formula is the same as that given in [9]:

$$\langle W_{R^0\pi^\pm \rightarrow \pi^\pm\tilde{\gamma}} V \rangle = \langle v\sigma_{R^0\pi} \rangle \simeq 1.5 \times 10^{-10} r \left[ \mu_8^2 \mu_S^{-4} C \right] \text{ mb.} \quad (13)$$

The factor  $C$  contains the uncertainty due to possible resonance effects and hadronic physics. Ref. [9] considered the range  $1 \leq C \leq 10^3$ . An analysis of the effect of the expected  $R_\pi$  resonance shows that  $C$  can exceed this by an order of magnitude (see Appendix), but we shall not dwell on this since our conclusions are mostly insensitive to the exact value of any large enhancement. However, for  $C/\mu_S^4 \lesssim 1$  the results are sensitive to the value of  $C/\mu_S^4$ . For reasons to be discussed in Section V, we also consider values of  $C$  as small as  $1/20$ .

Using Eq. (7) and  $n_j^{eq} \approx g_j(m_j T / (2\pi))^{3/2} e^{-m_j/T}$ , we then find

$$\begin{aligned} \langle W_{\tilde{\gamma}\pi^\pm \rightarrow \pi^\pm R^0} V \rangle n_{\pi^\pm}^{eq} &= \frac{n_{R^0}^{eq}}{n_{\tilde{\gamma}}^{eq}} n_{\pi^\pm}^{eq} \langle v\sigma_{R^0\pi} \rangle \\ &= 9.17 \times 10^{-13} r^{5/2} x^{-3/2} \exp(-0.175\mu_8^{-1}x) \text{ GeV} \\ &\quad \times \exp[-(r-1)x] \left[ \mu_8^{7/2} \mu_S^{-4} C \right]. \end{aligned} \quad (14)$$

Note in Eq. (14) that parameters  $C$  and  $\mu_S$  occur only together in the combination  $C/\mu_S^4$ , which we take to lie in the range

$$6.17 \times 10^{-4} \lesssim \frac{C}{\mu_S^4} \lesssim 10^4 \quad (15)$$

in accordance with the limit on  $\mu_S$  given by Table I and Eq. (1).

### B. The inverse decay reactions

We now estimate the decay rate of  $R^0$  and use Eq. (7) to obtain the inverse decay rate. If charge conjugation invariance is exact, two body decays of an  $R^0$  to a  $\tilde{\gamma}$  and a pseudoscalar meson ( $C=+1$ ) are forbidden [6]. In order to avoid reliance on a model of SUSY-breaking and its predictions for the extent of C-violation, we parameterize the branching fraction of an  $R^0$  to 2- and 3-body final states by  $b_2$  and  $b_3$ , respectively. As in the  $\tilde{\gamma} - R^0$  conversion reaction, the neutral pion channel ( $R^0 \rightarrow \tilde{\gamma}\pi^0\pi^0$ ) can be safely ignored even if  $b_3 \gg b_2$ . When  $b_2$  is not negligible, the two-body final states could be  $\tilde{\gamma}\pi^0$  and  $\tilde{\gamma}\eta$ . However, the matrix element-squared for  $R^0 \leftrightarrow \eta\tilde{\gamma}$  is about one-quarter of that for  $R^0 \leftrightarrow \pi^0\tilde{\gamma}$  [6], and the  $\eta$  final state is additionally suppressed by phase space. Hence we make an unimportant error by retaining only the two-body final state  $\tilde{\gamma}\pi^0$ . Thus, the two reactions of interest are  $R^0 \rightarrow \tilde{\gamma}\pi^+\pi^-$  and  $R^0 \rightarrow \tilde{\gamma}\pi^0$ , with branching fractions  $b_3$  and  $b_2$ , respectively. In this subsection, we show that our results depend only minimally upon the individual magnitudes of  $b_2$  and  $b_3$  because the Boltzmann equation depends only on the total decay width of the  $R^0$  and  $b_2 + b_3 \approx 1$  (due to the relative phase space suppression of 4-body decays).

The rates  $\Gamma(R^0 \rightarrow \tilde{\gamma}\pi^0)$  and  $\Gamma(R^0 \rightarrow \tilde{\gamma}\pi^+\pi^-)$  are obtained from the  $R^0$  decay rate in Ref. [9] by inserting  $b_2$  and  $b_3$  to get

$$W_{R^0 \rightarrow \tilde{\gamma}\pi^+\pi^-} = \Gamma_{R^0 \rightarrow \tilde{\gamma}\pi^+\pi^-} = 2.0 \times 10^{-14} \mathcal{F}(r)\theta(r - 0.350\mu_8^{-1} - 1) \text{ GeV} [\mu_8^5 \mu_S^{-4} B b_3] \quad (16)$$

and

$$W_{R^0 \rightarrow \tilde{\gamma}\pi^0} = \Gamma_{R^0 \rightarrow \tilde{\gamma}\pi^0} = 2.0 \times 10^{-14} \mathcal{F}(r)\theta(r - 0.175\mu_8^{-1} - 1) \text{ GeV} [\mu_8^5 \mu_S^{-4} B b_2] \quad (17)$$

where  $\mathcal{F}(r) = r^5(1 - r^{-1})^6$ ,  $\theta$  is a step function employed to model the threshold of the decay channel, and the factor  $B$  reflects the overall uncertainty which we set to be in

the range  $1/300 \lesssim B \lesssim 3$ . Having obtained the decay rate formula, we now use Eq. (7) to convert it to the inverse decay rate<sup>9</sup>

$$\langle W_{\tilde{\gamma}\pi^+\pi^-\rightarrow R^0} V^2 \rangle n_{\pi^+}^{eq} n_{\pi^-}^{eq} = \langle \Gamma_{R^0 \rightarrow \tilde{\gamma}\pi^+\pi^-} \rangle \frac{n_{R^0}^{eq}}{n_{\tilde{\gamma}}^{eq}} \quad (18)$$

$$= 2.0 \times 10^{-14} r^{3/2} \mathcal{F}(r) e^{-(r-1)x} \theta(r - 0.350\mu_8^{-1} - 1) \text{GeV} [\mu_8^5 \mu_S^{-4} B b_3], \quad (19)$$

and similarly

$$\langle W_{\tilde{\gamma}\pi^0 \rightarrow R^0} V \rangle n_{\pi^0}^{eq} = \langle \Gamma_{R^0 \rightarrow \tilde{\gamma}\pi^0} \rangle \frac{n_{R^0}^{eq}}{n_{\tilde{\gamma}}^{eq}} \quad (20)$$

$$= 2.0 \times 10^{-14} r^{3/2} \mathcal{F}(r) e^{-(r-1)x} \theta(r - 0.175\mu_8^{-1} - 1) \text{GeV} [\mu_8^5 \mu_S^{-4} B b_2]. \quad (21)$$

Combining Eqs. (19) and (21) with Eq. (12), and using  $b_2 + b_3 \approx 1$ , we find

$$R_{tot} = \Gamma_{tot} g(b_2, r, \mu_8) + 2 \langle W_{\tilde{\gamma}\pi^\pm \rightarrow \pi^\pm R^0} V \rangle n_{\pi^\pm}^{eq} \quad (22)$$

where  $\Gamma_{tot} \equiv 2.0 \times 10^{-14} r^{3/2} \mathcal{F}(r) e^{-(r-1)x} \text{GeV} [\mu_8^5 \mu_S^{-4} B]$  and

$$g(b_2, r, \mu_8) \equiv \begin{cases} 1 & \text{if } r > 0.35\mu_8^{-1} + 1 \\ b_2 & \text{if } 0.35\mu_8^{-1} + 1 \geq r > 0.175\mu_8^{-1} + 1 \\ 0 & \text{otherwise} \end{cases} .$$

The function  $g$  allows both the two and the three body decays when the  $R^0$  is sufficiently heavy ( $r > 0.35\mu_8^{-1} + 1$ ) but forbids the three body channel when the  $R^0$  mass drops below the two pion channel threshold. Thus, as long as the parameterization in Eqs. (19) and (21) is valid and the  $R^0$  is massive enough ( $r > 0.35\mu_8^{-1} + 1$ ) to allow kinematically three body decays, our results are independent of  $b_2$  and  $b_3$ , and hence the question of C

---

<sup>9</sup> A more accurate relationship between the thermal averaged decay rate and the non-thermal averaged decay rate is  $\langle \Gamma_{R^0 \rightarrow \tilde{\gamma}\pi^+\pi^-} \rangle = \Gamma_{R^0 \rightarrow \tilde{\gamma}\pi^+\pi^-} K_1(rx)/K_2(rx)$  where  $K_\nu$  is the modified Bessel function irregular at the origin. Since the freeze out occurs typically between  $x = 20$  and  $x = 30$ , the thermal averaged reaction rate will maximally deviate from the non-thermal averaged one when  $r = 1.1$  and  $x = 20$ . In that case  $K_1(rx)/K_2(rx) = 0.94$  which is still an insignificant correction. Thus we neglect this complication in our calculations.

invariance. Therefore, considerations of C invariance is generally unimportant for large values of  $r$ .

In these formulae, the squark mass parameter  $\mu_S$  occurs only in combination with the uncertainty parameter  $B$  in the form  $B/\mu_S^4$ . Using Table I and Eq. (1), we limit the decay rate for a given  $\mu_8$  and  $r$  to those values corresponding to the range<sup>10</sup>

$$4.12 \times 10^{-5} \lesssim \frac{B}{\mu_S^4} \lesssim 48. \quad (24)$$

### C. Self-Annihilations and co-annihilations

For the thermal averaged  $R^0$  self-annihilation cross section, we use  $\langle v\sigma_{R^0 R^0} \rangle = 31A$  mb. This is extracted from the  $p\bar{p}$  annihilation cross section in the comparable kinematic region[13] with a factor  $A$  inserted to cover a possible difference between  $R^0 R^0$  and  $p\bar{p}$  annihilation, and to account for the uncertainty due to possible resonance enhancements and other hadronic effects. We take  $A$  to lie in the range  $10^{-2} \lesssim A \lesssim 10^2$ .<sup>11</sup> Hence, the

---

<sup>10</sup>Because of our estimated upper and lower limit on each of the parameters  $C, B$ , and  $\mu_S$  separately (Eq. (15), Eq. (24), and Table I), for a given value of  $B/\mu_S^4$ , the allowed range of values for  $C/\mu_S^4$  given by Eq. (15) must be supplemented with the condition

$$\left[ \frac{C_{min}}{B_{max}} \right] \frac{B}{\mu_S^4} \lesssim \frac{C}{\mu_S^4} \lesssim \left[ \frac{C_{max}}{B_{min}} \right] \frac{B}{\mu_S^4} \quad (23)$$

where from Eq. (15)  $C_{max} = 1000$ ,  $C_{min} = 1/20$ , and  $B_{max} = 3$ , and  $B_{min} = 1/300$ .

<sup>11</sup>Note the absence of the  $v^2$  factor which appears in the familiar case of two identical Majorana spinors annihilating to a fermion-antifermion pair (e.g.,  $\tilde{\gamma}\tilde{\gamma}$  or  $\tilde{g}\tilde{g} \rightarrow q\bar{q}$ ). Like the  $\tilde{\gamma}\tilde{\gamma}$  and  $\tilde{g}\tilde{g}$  states, the  $R^0 R^0$  system must be antisymmetric by Fermi statistics, i.e.,  $^1S_0, ^3P_1, \dots$ . However typical final states of  $R^0 R^0$  annihilation (e.g., 3 pions) can have  $0^{-+}$  quantum numbers, allowing  $s$ -wave annihilation. This is to be contrasted with the usual case that the final state is a fermion-antifermion pair. Since the sfermion-fermion-gaugino interaction conserves chirality, the  $0^{-+}$  state in that case is helicity-suppressed and thus  $p$ -wave annihilation is necessary. This treatment departs from Ref. [9], but does not lead to significantly different conclusions than the  $\langle v\sigma_{R^0 R^0} \rangle = 100Av^2$  mb used there.

$R^0$  self-annihilation rate is given by

$$\langle W_{R^0 R^0 \rightarrow X} V \rangle n_{R^0}^{eq} = 10 A r^{3/2} x^{-3/2} \exp(-rx) [\mu_8^3] \text{GeV}. \quad (25)$$

Note that although the  $R^0$  self-annihilation rate is generally much larger than the other reaction rates before the  $\tilde{\gamma}$  freeze out time, it is usually not strong enough to maintain  $R^0$  in equilibrium abundance through the  $\tilde{\gamma}$  freeze out time. This fact, not taken into account in Ref. [9], leads to differences in the results between that paper and the present analysis.

The well known thermal average of the  $\tilde{\gamma}$  self-annihilation cross section [14,15,16,17] can be approximated as [9]  $\langle v \sigma_{\tilde{\gamma}\tilde{\gamma}} \rangle = 2.0 \times 10^{-11} x^{-1} [\mu_8^2 \mu_S^4]$  mb for our purposes, giving the transition rate

$$\langle W_{\tilde{\gamma}\tilde{\gamma} \rightarrow X} V \rangle n_{\tilde{\gamma}}^{eq} = 3.3 \times 10^{-12} x^{-5/2} \exp(-x) [\mu_8^5 \mu_S^{-4}] \text{GeV}. \quad (26)$$

Because the  $\tilde{\gamma}$  self-annihilation becomes ineffective earlier than the  $R^0$  self-annihilation, it contributes very little to our results.

In summary, the reactions that will be important to our system of equations are  $R^0 R^0 \leftrightarrow X$ ,  $R^0 \pi \leftrightarrow \tilde{\gamma} \pi$ ,  $R^0 \leftrightarrow \tilde{\gamma} \pi \pi$ , and  $R^0 \leftrightarrow \tilde{\gamma} \pi$ .

#### IV. GENERAL RESULTS

In this section, we impose the cosmological constraint  $\Omega_{\tilde{\gamma}} h^2 \leq 1$  on the integration results of the Boltzmann equation to identify the allowed region of the parameter space and use the condition  $\Omega_{\tilde{\gamma}} h^2 \geq 0.01$  to identify those parameters for which the photinos are significant dark matter candidates. The parameter space is spanned by  $r \equiv M/m$ ,  $B/\mu_S^4$ ,  $C/\mu_S^4$ ,  $\mu_8$ , and  $A$  (see Table I and Eqs. (1), (13), (16), and (25)). For reasons of physical interest, we will present our results in terms of the  $\tilde{\gamma}$  mass  $m$  and the

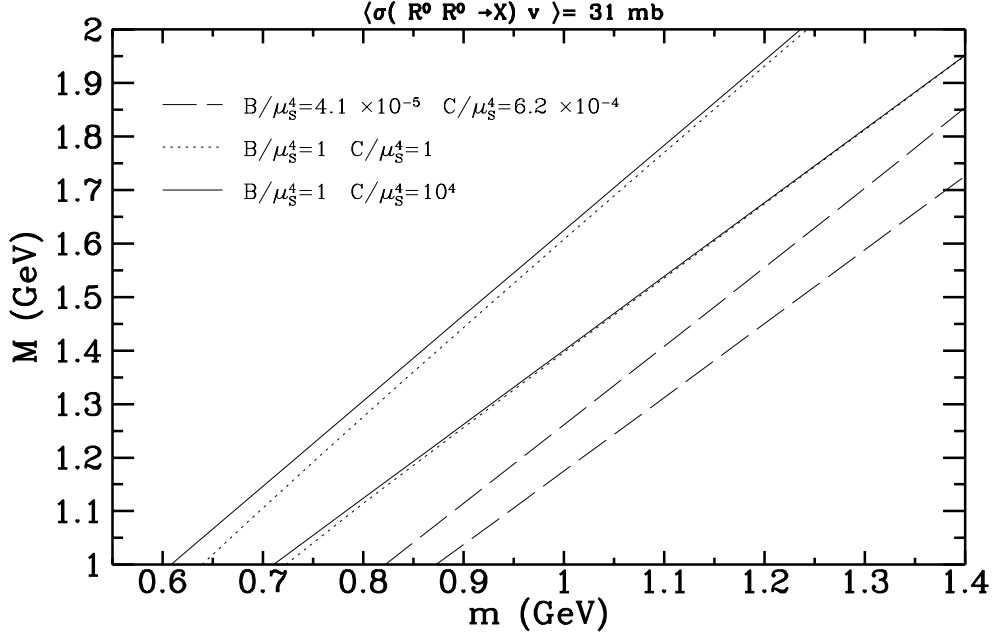


**Fig. 1:** For any given contour type, the left contour gives those values of  $M$  ( $R^0$  mass) and the  $m$  ( $\tilde{\gamma}$  mass) for which  $\Omega_{\tilde{\gamma}}h^2=1$  while the right one gives those for which  $\Omega_{\tilde{\gamma}}h^2 = 0.01$ . The region above the left contour is ruled out by the present analysis.

$R^0$  mass  $M$  instead of using  $r$  and  $\mu_8$ . We constrain the parameter space for the two extreme cases  $b_2 = 1$  and  $b_2 = 0$  (maximal C violation and C conservation, respectively), but in general, the results are insensitive to the value of  $b_2$ . As will be discussed below, among the parameters of the model, the relic abundance is most sensitive to the variations of  $r$ . Using a maximum  $A$  of about 100, our analysis gives us an upper bound of  $r \leq 1.8$ .

In Fig. 1, we show the Boltzmann equation integration results with exact C invariance ( $b_2 = 0$ ). For any given contour type, the left contour represents the  $\Omega_{\tilde{\gamma}}h^2 = 1$  contour while the right contour represents the  $\Omega_{\tilde{\gamma}}h^2 = 0.01$  contour. The present analysis thus excludes the region above the left contour and constrains the masses to lie between a given contour type in order for the  $\tilde{\gamma}$  to be a significant source of dark matter (defined by  $\Omega_{\tilde{\gamma}}h^2 \geq 0.01$ ). In this figure, the parameter  $A$  multiplying the  $R^0$  self-annihilation



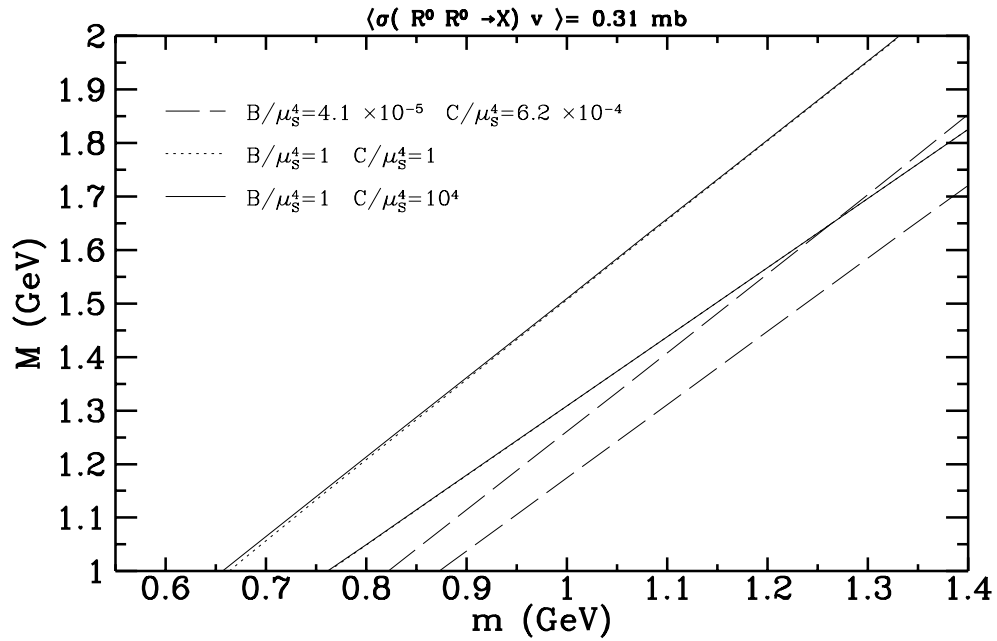
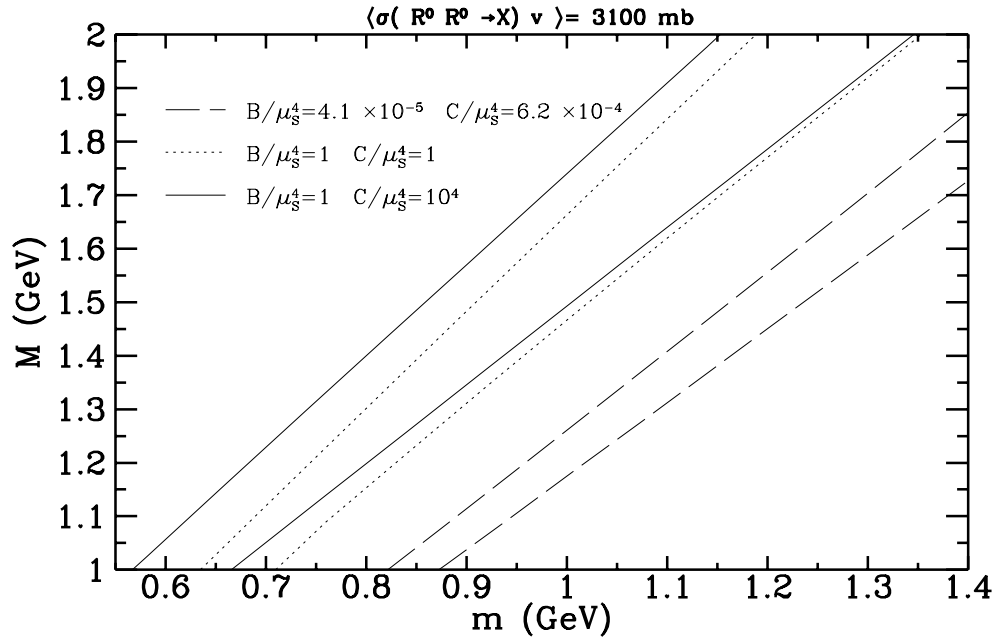


**Fig. 2:** Same as Fig. 1 except for the  $R^0$  self-annihilation cross sections. For the top figure,  $\langle v\sigma(R^0 R^0 \rightarrow X) \rangle = 3100 \text{ mb}$  while for the bottom figure,  $\langle v\sigma(R^0 R^0 \rightarrow X) \rangle = 0.31 \text{ mb}$ .

cross section has been set to 1.

Note that the values of  $r \equiv M/m$  are insensitive to  $C/\mu_S^4 \gtrsim 1$ . This can be heuristically understood by the fact that as  $C/\mu_S^4$  increases, the freeze out time (the time at which the  $\tilde{\gamma} - R^0$  conversion reaction rate becomes negligible compared to  $H$  if the  $\tilde{\gamma} - R^0$  conversion rate dominates over the inverse decay rate) approaches the time at which the  $R^0$  self-annihilation rate becomes negligible compared to  $H$ . Thus, as  $C/\mu_S^4$  increases, the photino abundance should approach the value for the limiting case when the  $R^0$  self-annihilation rate becomes negligible *before* the freeze out time. When the  $R^0$  self-annihilation rate becomes negligible, the number of SUSY particles are approximately conserved.<sup>12</sup> Thus, the  $\tilde{\gamma}$  abundance is largely determined by the time at which  $R^0$  self-annihilation becomes negligible in this limiting case. This time is determined by  $r$  and is independent of  $C/\mu_S^4$ .<sup>13</sup>

Because the extent of C violation affects the photino abundance only in the region  $0.14\text{GeV} \leq M - m \leq 0.28\text{GeV}$ , it is clear from Fig. 1 that only the long dashed contours (corresponding to small  $\tilde{\gamma} - R^0$  conversion and inverse decay rates) may depend on the extent of C violation. However, for this region,  $B/\mu_S^4$  is too small for the inverse decay reaction to play any significant role, and hence, our results are insensitive to the extent of C violation. Explicit numerical calculations confirm this.

In Fig. 2, we show the effect of changing the magnitude of the  $R^0$  self-annihilation cross section (by changing  $A$  in Eq. (25)). When we increase the magnitude from that of Fig. 1 by a factor of 100 (due to a possible resonance enhancement), the contours

---

<sup>12</sup>The  $\tilde{\gamma}$  self-annihilation rate is already negligible by the the time the  $R^0$  self-annihilation becomes negligible.

<sup>13</sup>This heuristic argument assumes that the  $R^0$  and  $\tilde{\gamma}$  abundances approximately follow a function independent of  $C/\mu_S^4$  until near the time that the SUSY particles become approximately conserved. This is of course true for the equilibrium abundance functions.

for  $C/\mu_S^4, B/\mu_S^4 \geq 1$  shift leftwards, and when we decrease the magnitude by a factor of 100, the same contours shift rightwards. In both cases, the contours corresponding to a small  $C/\mu_S^4$  and  $B/\mu_S^4$  (corresponding to small  $\tilde{\gamma} - R^0$  conversion and inverse decay rates) remain essentially unchanged. This is expected since for the shifted contours, the inverse decay and the  $\tilde{\gamma} - R^0$  conversion reaction rates are large enough such that the  $\tilde{\gamma}$  abundance is sensitive to the time at which the  $R^0$  self-annihilation becomes negligible (by the mechanism discussed before) while for the unchanging contours, the  $\tilde{\gamma}$  abundance is determined nearly independently of the time that  $R^0$  self-annihilation rate becomes negligible. When the inverse decay and the  $\tilde{\gamma} - R^0$  conversion reaction rates are very small as is the case for the unchanged contours, the  $\tilde{\gamma}$  freeze out time that will lead to  $\Omega_{\tilde{\gamma}} h^2 \gtrsim 0.01$  is much earlier than the time when the  $R^0$  self-annihilation reaction rates become negligible. Hence, near the  $\tilde{\gamma}$  freeze out time, the  $R^0$  self-annihilation reaction rate will dominate the  $dY_{R^0}/dx$ , the  $R^0$  abundance will be nearly in equilibrium, and the  $dY_{\tilde{\gamma}}/dx$  will decouple from  $dY_{R^0}/dx$ , leading to a  $\tilde{\gamma}$  freeze out value that is nearly independent of the  $R^0$  self-annihilation reaction. Note also that when the time at which the  $R^0$  self-annihilation becomes negligible is pushed away from the  $\tilde{\gamma}$  freeze out time by increasing the  $R^0$  self-annihilation cross section, the solid and the dotted contours become more sensitive to the value of  $C/\mu_S^4$  as we expect from our heuristic discussion above.

According to Fig. 2, the maximum value of  $r$  allowed by the condition that  $\Omega_{\tilde{\gamma}} h^2 \leq 1$  is about 1.8.

## V. CROSSING RELATION

The amplitudes determining the quantities  $\langle v\sigma \rangle \equiv \langle v\sigma_{R^0\pi^\pm \rightarrow \tilde{\gamma}\pi^\pm} \rangle$  and  $\Gamma_{tot}$  are related

through crossing symmetry if we associate  $\Gamma_{tot}$  with the C conserving  $R^0 \rightarrow \tilde{\gamma}\pi^+\pi^-$  transition rate (i.e., if we set  $b_2 = 0$ ). To obtain a useful constraint from the crossing relation, and to implement the constraints following from the symmetries of the underlying theory, we derive in this section an approximate effective interaction Lagrangian. If the  $R_\pi$  resonance is sufficiently far above threshold such that the  $R^0\pi^\pm \rightarrow \tilde{\gamma}\pi^\pm$  amplitude can be taken to be momentum independent for the purposes of the freeze-out calculation, a single parameter governs both  $\langle v\sigma_{R^0\pi^\pm \rightarrow \tilde{\gamma}\pi^\pm} \rangle$  and  $\Gamma_{tot}$ . This allows us to determine what ranges of  $R^0$  lifetime are most favorable for cosmology, in the event the  $R_\pi$  is too far above threshold to have a significant impact.

We first note that neglecting light quark masses as well as left-right squark-mass splitting in comparison to the squark masses, the four-Fermi effective operator governing  $R^0\pi \leftrightarrow \tilde{\gamma}\pi$  can be written in the current-current form

$$\mathcal{H}_{\text{int}} = i\kappa_V \lambda_g^a \gamma^\mu \lambda_{\tilde{\gamma}} \bar{q}^i \gamma_\mu T_{ij}^a q^j + \kappa_A \lambda_g^a \gamma^\mu \gamma_5 \lambda_{\tilde{\gamma}} \bar{q}^i \gamma_\mu \gamma_5 T_{ij}^a q^j \quad (27)$$

where  $\lambda_{\tilde{g}}$  and  $\lambda_{\tilde{\gamma}}$  are 4-component Majorana spinor fields for the gluino and photino,  $\{a, i, j\}$  are color indices, and the  $T^a$  are  $3 \times 3$  SU(3) matrices. This form follows because the underlying theory conserves the chirality of light quarks and their SUSY partners,<sup>14</sup> allowing only current-current couplings for the quarks to appear. Approximate degeneracy of the left-right squark masses then ensures parity conservation which, with Lorentz invariance, results in the form of Eq. (27). A direct calculation starting with the fundamental supersymmetric Lagrangian of course gives the form (27) and gives  $\kappa_V = 0$  and  $\kappa_A = g_S e_q e / M_S^2$ .<sup>15</sup> The vanishing of  $\kappa_V$  is due to C-conservation, since the

---

<sup>14</sup>Chirality conservation of the light quarks and their squarks is an excellent approximation in all SUSY models proposed to date, for which left-right squark mixing is proportional to the mass of the corresponding quark.

<sup>15</sup>The strong coupling constant is denoted by  $g_S$  and  $e_q$  gives the electric charge of the quark in units of positron charge  $e$ .

term it multiplies is C-odd for Majorana fields  $\lambda_{\tilde{\gamma}}$  and  $\lambda_{\tilde{\gamma}}$ .

We are concerned with estimating matrix elements such as  $\langle R^0 \pi | \mathcal{H}_{\text{int}} | \tilde{\gamma} \pi \rangle$ . The most general form of the matrix element includes current-current terms, plus other terms which result from the fact that the  $R^0$  is not pointlike and chirality flip can be induced by long-distance effects. However, since the  $R^0$  is expected to be more compact than ordinary hadrons (as is observed for the  $0^{++}$  glueball<sup>16</sup>), we neglect all but the current-current terms. Therefore we have  $\mathcal{L}_{\text{eff}} = i\kappa \overline{R^0} \gamma^\mu \lambda_{\tilde{\gamma}} J_\mu$ , where  $J_\mu$  is a C-odd,<sup>17</sup> four-vector pion current determined by chiral perturbation theory, and  $\kappa$  is of order  $\kappa_A$ . The single-pion contribution to  $J_\mu$  vanishes, and the two pion contribution is simply  $J_\mu = i(\pi^\dagger \partial_\mu \pi - (\partial_\mu \pi)^\dagger \pi)$ . In general,  $\kappa$  is a function of kinematic invariants, but far from resonances a constant should be a reasonable approximation.

Using  $\mathcal{L}_{\text{eff}}$  we can compute both  $\langle v\sigma \rangle \equiv \langle v\sigma_{R^0 \pi^\pm \rightarrow \tilde{\gamma} \pi^\pm} \rangle$  and  $\Gamma_{\text{tot}}$  in terms of the single parameter  $\kappa$ . Thus, for a given  $r$  and  $M$ ,  $\Omega_{\tilde{\gamma}} h^2$  is a function of the single parameter  $\kappa$ . Likewise, values for  $\{\Omega_{\tilde{\gamma}} h^2, r, M\}$  pick out a unique value of  $\kappa$ , which in turn determines  $\Gamma_{\text{tot}}$ . In Fig. 3, we assume  $\Omega_{\tilde{\gamma}} h^2 = 0.25$  (cosmologically “favored” value) and give the  $R^0$  lifetime for a range of  $r$  and  $R^0$  mass. We stress that these results are only indicative of the actual lifetime-mass-relic density relation, since the most general effective Lagrangian depends on additional parameters which we neglect here. Furthermore if the  $R_\pi$  resonance is sufficiently close to threshold to produce an enhancement effect, there is no simple relation among  $\Omega_{\tilde{\gamma}} h^2$ ,  $r$ , and the  $R^0$  lifetime, and Fig. 3 is not relevant. It is encouraging that the  $R^0$  lifetimes required to give the “correct” relic density is compatible with predictions [5] and also compatible with experimental limits [4].

It is also of interest to extract the values of  $B$  and  $C$  implied by  $\Omega_{\tilde{\gamma}} h^2 = 0.25$ ; this is shown in Fig. 4. Overall, these results suggest that the inverse decay reaction may

---

<sup>16</sup>D. Weingarten, private communication.

<sup>17</sup>Because the  $R^0$  and  $\tilde{\gamma}$  have opposite C quantum numbers [6].

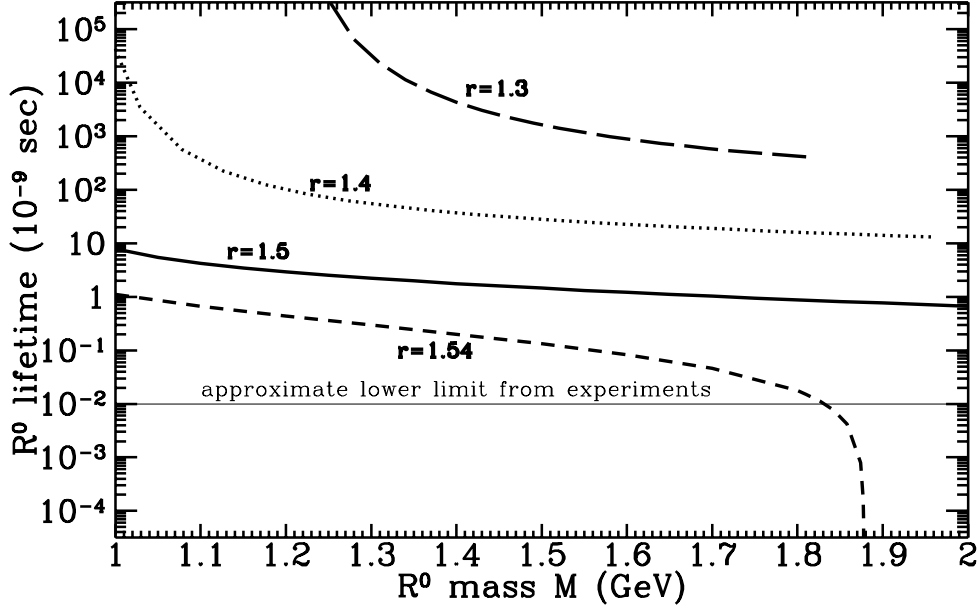


Fig. 3: The  $R^0$  lifetime that implies a cosmological photino abundance of  $\Omega_{\tilde{\gamma}} h^2 = 0.25$  is plotted as a function of the  $R^0$  mass and its ratio  $r$  to the photino mass. A model Lagrangian has been used to determine the crossing relation between the  $\tilde{\gamma} - R^0$  conversion amplitude and the  $R^0$  decay amplitude.

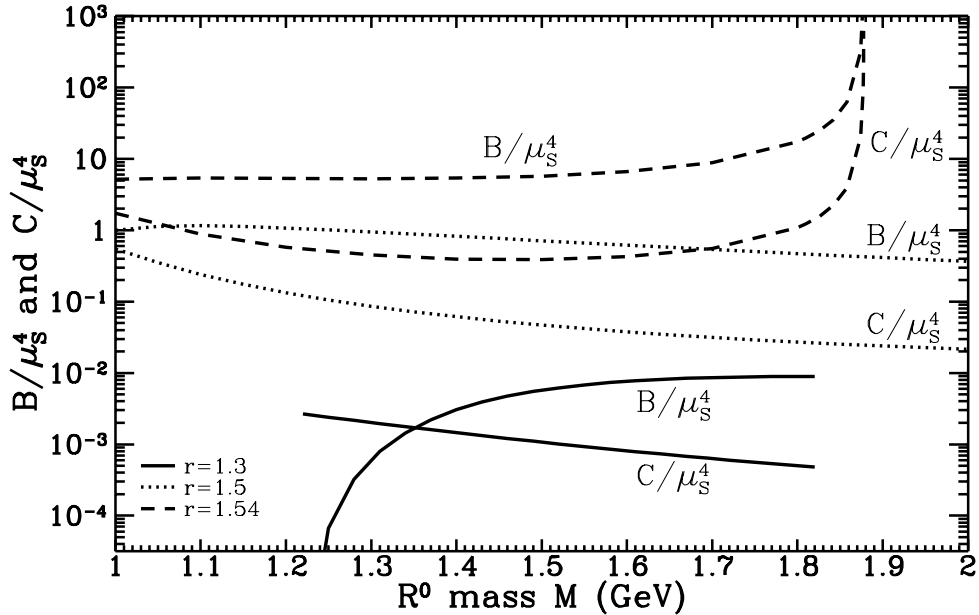


Fig. 4: The  $B/\mu_S^4$  and  $C/\mu_S^4$  values corresponding to the contours shown in Fig. 3 are plotted. The typical suppression of  $C/\mu_S^4$  with respect to  $B/\mu_S^4$  reflects the fact that both the  $\tilde{\gamma} - R^0$  conversion and the inverse decay reactions have comparable rates in our simple model which does not take into account possible resonance enhancements.

not be entirely negligible in determining the photino abundance if there is no resonance enhancement in the scattering reaction.

## VII. SUMMARY AND CONCLUSIONS

In this article, we have investigated the cosmological constraints on the physics of light photinos and gluinos. A full treatment of the Boltzmann equations governing the photino freeze out has been carried out, considering the total  $R^0$  width and  $R^0\pi \rightarrow \tilde{\gamma}\pi$  scattering cross section as independent quantities. We find that to avoid photino abundances inconsistent with cosmology, the ratio  $r$  of  $R^0$  mass to  $\tilde{\gamma}$  mass must be less than about 1.8. We checked that if the  $R^0$  is the LSP, its annihilation is too efficient for it to account for the observed dark matter density.

We also developed an approximate effective Lagrangian description of the  $R^0\pi \leftrightarrow \tilde{\gamma}\pi$  amplitude, neglecting possible C-violating and chirality-violating effects. If the  $R_\pi$  resonance is far above threshold,  $\mathcal{L}_{\text{eff}}$  is specified by a single parameter governing both the total  $R^0$  width and  $R^0\pi \rightarrow \tilde{\gamma}\pi$  scattering cross section. Assuming that the universe is at its critical density with photinos constituting most of the dark matter fixes this parameter for given  $R^0$  and  $\tilde{\gamma}$  masses. We therefore obtain the cosmologically favored lifetime range of the  $R^0$  as a function of its mass (shown in Fig. 3) in the absence of a low lying  $R_\pi$  resonance. The lifetime will be increased compared to the values given in Fig. 3 when the  $R_\pi$  resonance enhances the cosmological importance of the scattering cross section in comparison to the inverse decay. Although the limitations in this estimate must not be forgotten, it is encouraging that the range thus determined,  $\tau > 10^{-10}\text{s}$ , is compatible with experimental limits [4]. Much of this range of lifetimes should be accessible to direct observation in upcoming experiments [6].

In closing, we note that detectability of relic dark matter is different for light  $\tilde{\gamma}$ 's than in the conventional heavy WIMP scenario for two reasons. Firstly, the usual relation between the relic density and the WIMP-matter scattering cross section only applies when the relic density is determined by the WIMP self-annihilation cross section, whereas in the light photino scenario it is determined by the  $\tilde{\gamma} - R^0$  conversion cross section,  $R^0$  self-annihilation cross section, and the  $\pi^\pm$  density at freeze out. Secondly, WIMP detectors have generally been optimized to maximize the recoil energy for a WIMP mass of order 10 to 100 GeV. Goodman and Witten in Ref. [18] discuss  $\tilde{\gamma}$  detection through  $\tilde{\gamma}$ -nucleon elastic scattering. Using Eq. (3) of Ref. [18] and the parameters discussed here, one finds that event rates range somewhere between  $10^{-3}$  and 10 events/(kg day). Unfortunately even if the event rate were larger, observation of relic light photinos would be difficult with existing detectors because the sensitivity of a generic detector is poor for the less than 1 GeV mass relevant in this case.

## ACKNOWLEDGMENTS

DJHC and EWK were supported by the DOE and NASA under Grant NAG5-2788. GRF was supported by the NSF (NSF-PHY-94-2302).

## APPENDIX

In this Appendix, we give the formalism for treating the resonance enhancement of the  $R^0\pi \rightarrow \tilde{\gamma}\pi$  cross section, using a Breit-Wigner form for the resonance. This permits us to assess the plausibility of the original range used in Ref. [9],  $C < 1000$ . We find that the effective value of  $C$  could be significantly larger than the originally estimated upper



bound, but this is only relevant if  $\langle v\sigma_{R^0R^0} \rangle$  is large enough that  $R^0$ 's remain in thermal equilibrium until after photino freeze out. As discussed in Section IV, this is not the case for large  $C$ , given our estimated  $\langle v\sigma_{R^0R^0} \rangle$ . However if there were a  $0^{-+}$  glueball near  $R^0R^0$  threshold, the  $R^0$ 's could stay in equilibrium to a lower temperature, and make it necessary to include resonance effects for both self-annihilation and  $\tilde{\gamma} - R^0$  conversion processes. We treat below the modeling of a resonance in the  $R^0\pi \rightarrow \tilde{\gamma}\pi$  reaction; the treatment of a resonance in the  $R^0R^0$  self-annihilation cross section is a close parallel.

The resonance relevant to the  $R^0\pi \rightarrow \tilde{\gamma}\pi$  reaction is called  $R_\pi$  which is composed at the valence level of  $\tilde{g}$ ,  $q_1$ , and  $\bar{q}_2$  (where  $q_i$ 's are  $u$  and  $d$  quarks). To study the maximum enhancement, we consider the  $R_\pi$  mass to be close to the  $R^0$  mass. We also consider here only the charged  $R_\pi$ 's since we are concerned with charged pion scattering (see Section III). Furthermore, because the  $s$ -wave contribution dominates, we restrict ourselves to the  $J = 1/2$  state.

We write the resonant contribution to the  $R^0\pi \rightarrow \tilde{\gamma}\pi$  cross section as

$$\sigma_{\text{res}} = \left[ \frac{4\pi}{p_{cm}^2} \right] \frac{m_{R_\pi}^2 \Gamma(R_\pi \rightarrow \tilde{\gamma}\pi)\Gamma(R_\pi \rightarrow R^0\pi)}{(m_{R_\pi}^2 - s)^2 + m_{R_\pi}^2 \Gamma_{tot}^2}, \quad (28)$$

where  $p_{cm}$  is the center of mass three-momentum of the incoming particles,  $s$  is the square of center of mass energy,  $m_{R_\pi}$  is the mass of  $R_\pi$ , the  $\Gamma(A \rightarrow BC)$ 's are momentum ( $s$ ) dependent widths to the incoming and outgoing channels,<sup>18</sup> and  $\Gamma_{tot}$  is the momentum dependent total width of the  $R_\pi$ . Thus, Eq. (13) becomes  $\langle v\sigma_{R^0\pi} \rangle = \langle v\sigma_{\text{nonres}} \rangle + \langle v\sigma_{\text{res}} \rangle$  where  $\langle v\sigma_{\text{nonres}} \rangle$  is the formula given in Eq. (13) with  $C$  set to a value of order 1. Since we are concerned with the maximum cross section resulting from the resonance, we are focusing on the region of parameters for which the non-resonant cross section is unimportant (i.e.  $\langle v\sigma_{\text{nonres}} \rangle \ll \langle v\sigma_{\text{res}} \rangle$ ).

---

<sup>18</sup>Note that  $C$  poses no relevant constraints on the decays of the charged  $R_\pi$  so both  $R_{\pi^\pm} \rightarrow R^0\pi^\pm$  and  $R_{\pi^\pm} \rightarrow \tilde{\gamma}\pi^\pm$  are allowed even though the  $R^0$  and  $\tilde{\gamma}$  have opposite  $C$  eigenvalues.

The kinematic momentum dependence of  $\Gamma(A \rightarrow BC)$  can be seen by expressing it in terms of a solid angle integral over the invariant amplitude squared  $|\mathcal{M}|^2$ :

$$\Gamma(A \rightarrow BC) = \left[ p_{cm}(s)/(32\pi^2 m_{R_\pi} \sqrt{s}) \right] \int d\Omega |\mathcal{M}(A \rightarrow BC)|^2. \quad (29)$$

Here  $p_{cm}(s) = 1/2\sqrt{(s - (m_B + m_C)^2)(s - (m_B - m_C)^2)}/s$  is the center of mass frame three-momentum of the decay products  $B$  and  $C$ . Defining  $4\pi\xi_B \equiv \int d\Omega |\mathcal{M}(A \rightarrow BC)|^2$  and assuming that  $\Gamma_{tot} \approx \Gamma(R_\pi \rightarrow R^0\pi)$ , the three independently adjustable parameters for the resonance are taken to be  $m_{R_\pi}$ ,  $\xi_{R^0}$ , and  $\xi_{\tilde{\gamma}}$ .

Since  $R_\pi \rightarrow R^0 + \pi$  is a strong decay, we can take its matrix element to be similar to the matrix element for some known strongly decaying resonance whose decay has no angular momentum barrier, for instance the  $f_0(1370)$  whose total width is 300-500 MeV[19]. Thus we use  $\xi_{R^0} \approx 16\pi \Gamma(f_0(1370)) m_{f_0(1370)} = 7.4 \text{ GeV}^2$ .

To determine  $\xi_{\tilde{\gamma}}$  we estimate the ratio of  $R_\pi \rightarrow \tilde{\gamma}\pi$  and  $R_\pi \rightarrow R^0\pi$  matrix elements by keeping track of the factors entering the short distance operator responsible for  $R^0 \rightarrow \pi\pi\tilde{\gamma}$ , namely  $\tilde{\gamma}\tilde{g}q\bar{q}$ . We use the  $R^0$  mass,  $M$ , to set the scale. This gives

$$\xi_{\tilde{\gamma}}/\xi_{R^0} = A e^2 \frac{\alpha_s(M_S)M^4}{\alpha_s(M)M_S^4} \approx A 4 \times 10^{-10} r^4 \mu_8^4 \mu_S^{-4}. \quad (30)$$

We define  $C_e$  to be the effective value of  $C$  in Eq. (13) that would reproduce the  $\Omega_{\tilde{\gamma}}h^2$  calculated using the present resonance model for a given set of resonance parameters, and taking  $A$  large enough to keep the  $R^0$  in equilibrium abundance until after photino-freeze out. To calculate the thermal average  $\langle v\sigma_{\text{Res}} \rangle$  of the resonant cross section, we use a non-relativistic approximation which is within a factor of two or better of the exact average. It can be expressed in terms of the one-dimensional integral

$$\langle v\sigma_{\text{Res}} \rangle = x^{3/2} \sqrt{\frac{8}{\pi} \left( \frac{\mu_8}{0.175} + \frac{1}{r} \right)} \int_0^\infty d\beta \beta \sigma(s(\beta)) e^{-\beta x} \quad (31)$$

where  $s(\beta) \approx 0.64\mu_8^2(r + 0.175/\mu_8)(r + 0.175/\mu_8 + 2\beta) \text{ GeV}^2$ .

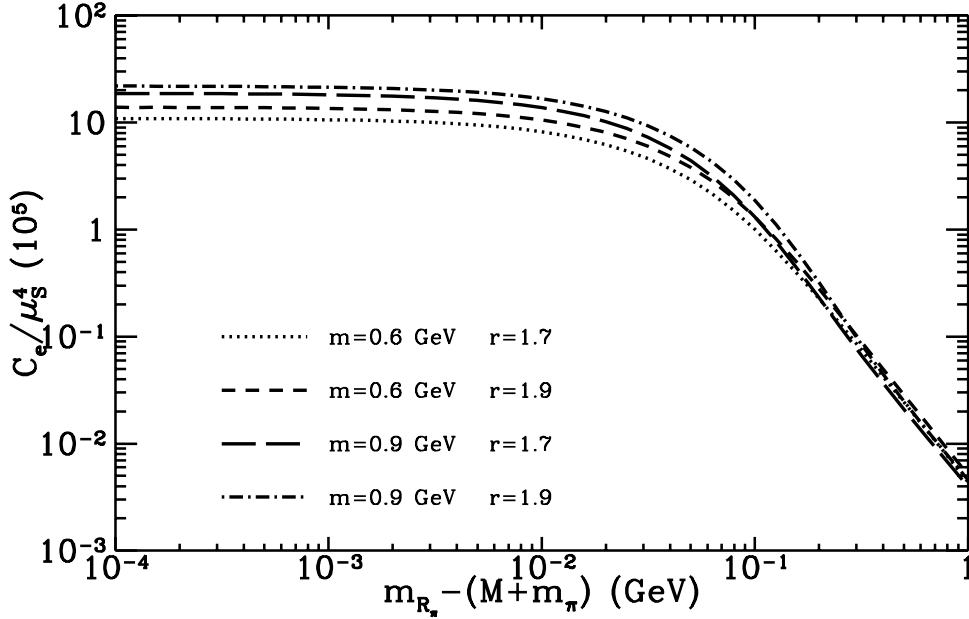


**Fig. 5:** The effective resonance enhancement factor  $C_e/\mu_S^4$  is shown as a function of  $r$ ,  $m$ , and  $m_{R_\pi}$ .

$C_e$  is largest when the resonance is near the threshold of the  $R^0\pi$  channel, because near the threshold  $\Gamma(R_\pi \rightarrow R^0\pi)$  is phase space suppressed in comparison to  $\Gamma(R_\pi \rightarrow \tilde{\gamma}\pi)$  and the peak value of the Breit-Wigner cross section is proportional to  $\sim \Gamma(R_\pi \rightarrow \tilde{\gamma}\pi)/\Gamma(R_\pi \rightarrow R^0\pi)$ . However, because the width of the resonance vanishes as  $m_{R_\pi}$  approaches threshold, the thermal average integral of the Breit-Wigner cross section does not grow arbitrarily large.

In order to assess the plausibility of the original range used in Ref. [9], we plot (Fig. 5)  $C_e/\mu_S^4$  as a function of  $r$ ,  $m$ , and  $m_{R_\pi}$  with  $A = 1$  (in Eq. (30)) and  $\mu_S = 1/2$ . In all of the  $m$  and  $r$  cases shown,  $C_e/\mu_S^4 \gtrsim 2 \times 10^5$  (or equivalently  $C_e \gtrsim 10^4$ ) when  $m_{R_\pi} - M - m_\pi \lesssim 70$  MeV. Since the mass splitting can easily be less than 70 MeV, we see that the  $C$  range used in Ref. [9] would be inadequate, were self-annihilation to be significantly larger than the non-resonant estimate adopted here.

- 
- [1] R. Barbieri and L. Girardello and A. Masiero, Phys. Lett. **127B**, 429 (1983); R. Barbieri and L. Maiani, Nucl. Phys. **B243**, 429 (1984).
- [2] G. R. Farrar and A. Masiero, Technical Report RU-94-38 (hep-ph/9410401), Rutgers Univ., 1994.
- [3] D. Pierce and A. Papadopoulos, Nucl. Phys. **B430**, 278 (1994).
- [4] G. R. Farrar, Phys. Rev. D **51**, 3904 (1995).
- [5] G. R. Farrar, Technical Report RU-95-17 (hep-ph/9504295), RU-95-25 (hep-ph/9508291), and RU-95-26 (hep-ph/9508292), Rutgers Univ., 1995.
- [6] G. R. Farrar, Phys. Rev. Lett. **76**, 4111 (1996).
- [7] The ALEPH Collaboration, Technical Report CERN-PPE-97/002, CERN, 1997.
- [8] B. Gary, CTEQ Workshop, FNAL, Nov. 1996; G. R. Farrar, Rencontres de la Valee d'Aoste, La Thuile, Feb. 1997 (preprint in preparation).
- [9] G. R. Farrar and E. W. Kolb, Phys. Rev. D **53**, 2990 (1996).
- [10] G. R. Farrar, Phys. Rev. Lett. **76**, 4115 (1996).
- [11] P. Gondolo and G. Gelmini, Nucl. Phys. **B360**, 145 (1991).
- [12] E. W. Kolb and M. S. Turner, *The Early Universe*, (Addison-Wesley, Redwood City, Ca., 1990).

- [13] Agnello et al., Phys. Lett. **256B**, 349 (1991).
- [14] H. Goldberg, Phys. Rev. Lett. **50**, 1419 (1983).
- [15] J. Ellis, J. S. Hagelin, D. V. Nanopoulos, K. Olive, and M. Srednicki, Nucl. Phys. **B238**, 453 (1984); G. B. Gelmini, P. Gondolo, and E. Roulet, Nucl. Phys. **B351**, 623 (1991); K. Griest, Phys. Rev. D **38**, 2357 (1988); L. Rozkowski, Phys. Lett. **262B**, 59 (1991).
- [16] J. Silk, K. Olive, and M. Srednicki, Phys. Rev. Lett. **53**, 624 (1985); T. K. Gaisser, G. Steigman, and S. Tilav, Phys. Rev. D **34**, 2206 (1986); J. S. Hagelin, K. W. Ng, and K. A. Olive, Phys. Lett. **180B**, 375 (1987); M. Srednicki, K. A. Olive, and J. Silk, Nucl. Phys. **B279**, 804 (1987).
- [17] G. L. Kane and I. Kani, Nucl. Phys. **B277**, 525 (1986); B. A. Campbell *et al.*, Phys. Lett. **173B**, 270 (1986).
- [18] M. W. Goodman and E. Witten, Phys. Rev. D **31**, 3059 (1985).
- [19] Particle Data Group, Phys. Rev. D **54**, 1 (1996).